ELSEVIER

Fuel Processing Technology 86 (2005) 617–640

FUEL PROCESSING TECHNOLOGY

www.elsevier.com/locate/fuproc

Simulation of petcoke gasification in slagging moving bed reactors

Soumitro Nagpal*, T.K. Sarkar, P.K. Sen

Research and Development Center, Engineers India Limited, Gurgaon 122001, India

Received 30 November 2003; received in revised form 30 May 2004; accepted 30 May 2004

Abstract

A mathematical model for simulation of moving bed petcoke gasifiers was developed. The model introduces a new feed characterization method, gas-phase resistance and volatilization models. The model is validated using reported data for a slagging gasifier. Effect of feed oxygen-to-coke and steam-to-coke ratios and feed coke rates on gasification performance was examined. Slagging zone moving bed gasifier operation with very high petcoke fluxes of over 4000 kg/m^2/h was possible with high petcoke conversion. Peak gas temperatures exceeded 1500 °C. Fluxes higher than 5000 kg/m^2/h are limited by an approach to fluidization of small particles in the combustion zone. The moving bed gasifier performance was found superior to performance of an entrained flow gasifier (EFG) with respect to energy efficiency and oxygen consumption.

Keywords: Gasification; Petcoke; Moving bed; Simulation; Kinetics

1. Introduction

Integrated gasification combined cycle power (IGCC) projects are gaining increasing acceptance, and worldwide installed capacity is increasing steadily [1]. New gasification plants have used both solid and liquid fuels as feed, and gasification methods employed include entrained flow, fluidized bed, and moving bed reactors. Petroleum refineries

* Corresponding author.

0378-3820/$ - see front matter © 2004 Elsevier B.V. All rights reserved.
doi:10.1016/j.fuproc.2004.05.012

produce large quantities of high sulfur petcoke and liquid fuel oils, which can be used as gasifier feedstock. Syngas from gasification units can also satiate the increasing hydrogen demand of refineries. Thus, refiners worldwide are considering the use of IGCC for meeting refinery energy and hydrogen demand.

Several commercial technologies are already available for gasification of petcoke in entrained flow reactors (EFG) [2–4]. However, very little is reported on the possibility of petcoke gasification in moving bed reactors (MBG), although these reactors are in use for various types of coal- and refuse-derived fuel gasification [32]. We have carried out a study to evaluate the feasibility of petcoke gasification in pressurized moving bed reactors. A simulation model was developed. The model was used to study gasifier performance with variation of oxygen, steam, and coke feed rates and feed oxygen concentration and to compare with petcoke gasification in entrained flow gasifiers with respect to syngas composition, reactor gas/solid temperatures, oxygen and steam consumption, etc.

Moving bed gasifier models have appeared in the literature for coal gasification since the late 1970s. The model presented here is based on earlier work reported by Yoon et al. [5], Adanez and Labiano [6], Hobbs et al. [7], Biba et al. [8], and Neogi et al. [9]. The salient features of our model are two-compartment feed solid characterizations based on proximate and ultimate analyses, separate gas and solid temperatures, axially uniform gas/solid phase plug flow, uniform bed porosity, volatilization kinetics, reaction chemistry, and petcoke/char kinetic parameters from earlier literature reports. The primary distinguishing features of our model are the feed characterization method, the mass-transfer resistance model, and the volatilization model.

2. Feed solid characterization

Coal and petcoke feed are typically characterized by their proximate and ultimate analyses. In the present model, we have chosen to characterize the feed solid carbon using a two-compartment model. The two compartments are chosen to have empirical formulae $CH_xSz_sN_{zn}$ and CH_yO_{zo} and represent fixed carbon and volatile carbon, respectively. This is a fairly simple compartmentalization but was found to be satisfactory for the petcoke simulations. The proximate and ultimate analyses are used to determine the fractions of fixed and volatile carbon and the coefficients for sulfur, nitrogen, and oxygen in the above empirical formulae. The distribution of hydrogen between fixed and volatile carbon is independently set based on the type of feed. For example, for a typical petcoke, the weight fraction hydrogen in fixed carbon can be ~0.7, while for a lignite coal, it can be significantly lower at ~0.1. Table 1 shows the fixed and volatile carbon molecularity calculated by this method.

3. Gasification and volatilization reaction scheme

The model components comprising feed solids are fixed and volatile carbon, ash, and moisture. Fig. 1 shows the fixed and volatile carbon combustion, gasification, and

Table 1
Feed characterization for typical lignite and petcoke from proximate and ultimate analyses

	Lignite	Petcoke
Proximate analysis (wt.%)		
Volatile carbon	25.3	9.6
Fixed carbon	32.9	80.6
Ash	36.2	0.5
Ultimate Analysis (wt.%)		
Carbon	44.20	89.23
Hydrogen	2.76	3.59
Nitrogen	0.70	1.35
Oxygen	9.76	0.10
Sulfur	0.76	5.22
H_2 in fixed carbon	10%	70%
Feed molecularity		
Fixed carbon	$CH_{0.10}S_{0.0091}N_{0.0196}$	$CH_{0.38}S_{0.0245}N_{0.0145}$
Volatile carbon	$CH_{2.28}O_{0.5610}$	$CH_{1.36}O_{0.0079}$

volatilization reaction scheme used in our model. The fixed carbon undergoes combustion, gasification, and hydro-pyrolysis reactions. H_2S, NH_3, and N_2 are assumed to form in association with fixed carbon gasification. Depending on fixed carbon stoichiometry, H_2S and NH_3 formation may consume some H_2 in addition to what is present in fixed carbon. Ash is assumed to be chemically inert but can liquefy in the slagging zone of the gasifier.

Solid volatile carbon is assumed present in two forms, as a gas-forming fraction and as a tar-forming fraction. The gas-forming fraction volatilizes to methane, CO_2, CO, and H_2, while the tar-forming fraction transmutes to tar. Tar formed in turn volatizes to soot and to

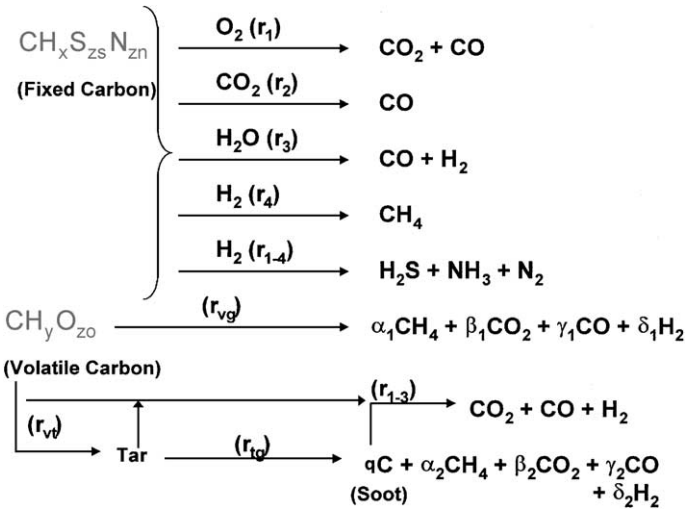

Fig. 1. Schematic of fixed and volatile carbon combustion, gasification, and volatilization reactions considered in model.

methane, CO_2, CO, and H_2. This devolatilization model is based on a scheme given by Bliek et al. [10]. We have assumed that fixed carbon, volatile carbon, tar, and soot can all undergo combustion and gasification reactions, in addition to the above devolatization reactions.

4. Fixed carbon combustion and gasification: chemistry and kinetics

The complete set of reactions that have been used to characterize the combustion and gasification of fixed carbon are shown in Fig. 1. In the following section, the fixed carbon is shown simply as C because the model assumes that fixed carbon constituents C and N, S, and H are distinct entities. N, S, and H in fixed carbon are assumed to gasify to H_2S, NH_3, and N_2 in proportion to C gasification.

The combustion of fixed carbon to CO_2 and CO are highly exothermic reactions. Carbon monoxide formation is reported favored at higher temperatures. The net reaction can be represented as

$$C+1/\lambda\ O_2\text{–}(r_1)\rightarrow 2(1-1/\lambda)CO+(2/\lambda-1)CO_2\ \Delta H=-123 \text{ to } -393 \text{ kJ/mol} \quad (1)$$

Laurendeau [11] correlated the relative preponderance of the CO versus CO_2 by

$$CO/CO_2=A\ e^{-E/RT}=2(\lambda-1)/(2-\lambda) \quad (2)$$

where $A=10^{3.5}$ and E=50–80 kJ/mol at high pressures.

The two carbon gasification reactions are the Boudouard reaction with CO_2 and steam gasification. These are endothermic reactions.

$$C+CO_2\text{–}(r_2)\rightarrow 2CO \qquad \Delta H=+170 \text{ kJ/mol} \quad (3)$$

$$C+H_2O\text{–}(r_3)\rightarrow CO+H_2\ \Delta H=+135 \text{ kJ/mol} \quad (4)$$

The heat released from the combustion reaction drives these gasification reactions. The gasification reactions are important in that they allow reduction in the net oxygen consumed in the process and produce the energy rich syngas components CO and H_2.

The final gasification reaction considered is the methane formation or hydro-pyrolysis reaction.

$$C+2H_2\text{–}(r_4)\rightarrow CH_4\ \Delta H=-80 \text{ kJ/mol} \quad (5)$$

The above reactions have been commonly used in previous modeling studies to represent char combustion and gasification. Several other important reactions between the major species can occur [12], e.g., char steam gasification to form methane and CO/CO_2. However, these reactions are derivable from the reaction set considered here.

Kinetics of the combustion and gasification reactions was modeled with Arrhenius/power law temperature dependence. The kinetic parameters for char and petcoke were obtained from several literature sources and are listed in Table 2. Rates for coal char combustion and gasification are widely reported. Denn and Shinnar [12] compared various char reaction rate

Table 2
Combustion and gasification kinetic parameters

Source	E_a (kJ/mol)	$k_{0,1}$ (m/h/K^N)	N
Char and petcoke combustion			
Sargent and Smith [13] (Bituminuous), Adanez and Labiano [6]	112.86	1.025E5	1
Hobbs et al. [7] (LigniteA)	85.63	4.392E3	1
Walsh and Green [17]			
Petcoke-Needle	171.38	4.510E9	0
Petcoke-Sponge	112.86	9.360E5	0
Tyler [15]			
Petcoke	158.60	2.128E8	0
Char and petcoke CO_2 gasification			
Hobbs et al. [7] (LigniteA)	129.70	1.231E4	1
Brown et al. [19] (Lignite)	165.00	4.428E4	1
Brown et al. [19] (UtahBit)	162.00	1.584E4	1
Dutta et al. [20]	246.62	9.922E6	1
Char steam gasification			
Brown et al. [19] (Lignite)	240.00	7.488E5	1
Brown et al. [19] (UtahBit)	147.00	4.788E3	1
Gibson and Euker [14]	175.56	1.804E5	1
Shift reaction			
Biba et al. [8]	12.56	1.000E7	0
Bhattacharya et al. [24]	40.70	1.065E0	2
Sohn and Braun [25]	60.69	1.350E9	0
Bustamante et al. [33] (reverse shift)	213.18	6.480E11	0

Overall rate constant, $k_i = k_{o-i} T^N e^{-Ea/RT}$.

data and projected the data of Sargent and Smith [13] for combustion and that of Gibson and Euker [14] for steam gasification, as typical. These rate parameters were also used in several earlier studies on coal/coke gasification modeling studies, including those of Yoon et al. [5], Biba et al. [8], and Adanez and Labiano [6]. Yoon et al. [5] were able to predict a slagging gasifier plant performance for coke well, using char kinetic parameters.

Intrinsic combustion rates of petcoke in oxygen over a temperature range 500–2000 °C have been obtained and reported by Australia's CSIRO divison of fossil fuels [15,16]. These studies compared the intrinsic reactivity (kg/m^2/s) of carbons from various sources including petcoke, brown, bituminous, and lignite coal chars. The intrinsic reactivity of petcoke was reported to be higher than that of all other carbons! Walsh and Green [17] reported petcoke combustion rates in oxygen at 550 °C. They used various types of coke produced in petroleum refineries: sponge- and needle-type delayed coke and fluid coke. They measured an activation energy of 112.8 kJ/mol for fluid coke and delayed sponge coke, while a higher activation energy of 171.4 kJ/mol was obtained for delayed needle coke. They concluded that the higher reactivity of fluid and delayed sponge coke at these temperatures was due to the catalytic effect of high metals concentration in these cokes, and at higher temperatures, kinetics of all three types of coke would follow those of needle coke. Several kinetic parameters for coal char and petcoke are listed in Table 2. Comparison of the combustion rate constants indicates higher char kinetics than petcoke,

especially at lower temperatures. Petcoke have lower a specific surface area (m^2/kg) vis-à-vis coals, leading to the lower reactivity (m/h or kg/kg/s). We used the kinetic parameters of petcoke from Tyler [15] in the model.

Tyler and Smith [18] reported petcoke CO_2 gasification kinetics at 700–900 °C. These kinetics are compared with coal char kinetics reported by Hobbs et al. [7], Brown et al. [19] (Lignite/UtahBit), and Dutta et al. [20] in Table 2. The petcoke rate constant/reactivity is seen to be significantly lower than that of all the chars. The Tyler and Smith [18] kinetic parameters were used in the model.

Kinetic parameters for petcoke steam-gasification reaction have been reported by Kairaitis and Tyler [21]. We did not have access to this paper and have used char kinetic parameters in the model. Kinetic parameters for char steam-gasification reaction from various sources are listed in Table 2. The rates of Gibson and Euker [14] and Brown et al. [19] (UtahBit) are quite similar, while that of Brown et al. [19] (Lignite) is seen to be lower especially at lower temperatures. Revankar et al. [22] reported petcoke steam-gasification rate constants determined at 800–850 °C. Their petcoke kinetic data agreed well with those of Gibson and Euker [14] at 800 °C. We have used the Brown et al. [19] (Lignite) parameters in the model because they give lower kinetics than the other char parameters.

The hydro-pyrolysis reaction is significantly slower than the other reactions discussed above and of minor significance in overall gasification performance. We used Biba et al.'s [8] kinetic parameters for this reaction, who reported E_a=230.274 kJ/mol and $K_{o,4}$=7.5 E 6 m/h.

Fig. 2 compares the rate constants of the combustion and gasification reactions used in this modeling study. The combustion reaction rate is seen to be the highest followed by the steam and CO_2 gasification. The figure also shows the mass-transfer rate estimated using the correlation of Gupta and Thodos [23]. Petcoke combustion rate is seen to become mass-transfer limited at temperatures in excess of 1150 °C, while the steam and CO_2 gasification kinetics are not mass-transfer limited at temperatures as high as 1400 °C.

4.1. Gas phase reactions

The water gas shift (WGS) reaction is an important reaction controlling the syngas composition in gasifiers. The reaction is fast enough at temperatures in excess of 1000 °C to be considered to be at equilibrium. However, at lower temperatures, the equilibrium assumption is invalid. The WGS reaction rate was modeled using the expression

$$r_5 = k_5(C_{CO}C_{H_2O} - C_{CO_2}C_{H_2}/K_{WGS}) \quad (6)$$

where k_5 is the temperature-dependent forward rate constant and K_{WGS} is the WGS reaction equilibrium constant. The shift equilibrium constant was taken from Yoon et al. [5]. The shift equilibrium favors CO at high temperatures and CO_2 at low temperatures. The equilibrium constant (K_{WGS}) is 1.37 at 727 °C and 134 at 227 °C.

The shift forward reaction rate parameters from several papers are shown in Table 2. The forward reaction kinetics given by Bhattacharya et al. [24] and Sohn and Braun [25] drop sharply at temperatures below 500 °C. Bustamante et al. [33] reported the reverse shift reaction rate in the temperature range 800–925 °C. We converted their rate into a forward rate by using K_f=$K_r^*K_{WGS}$. We have used the kinetic parameters of Bhattacharya et al. [24].

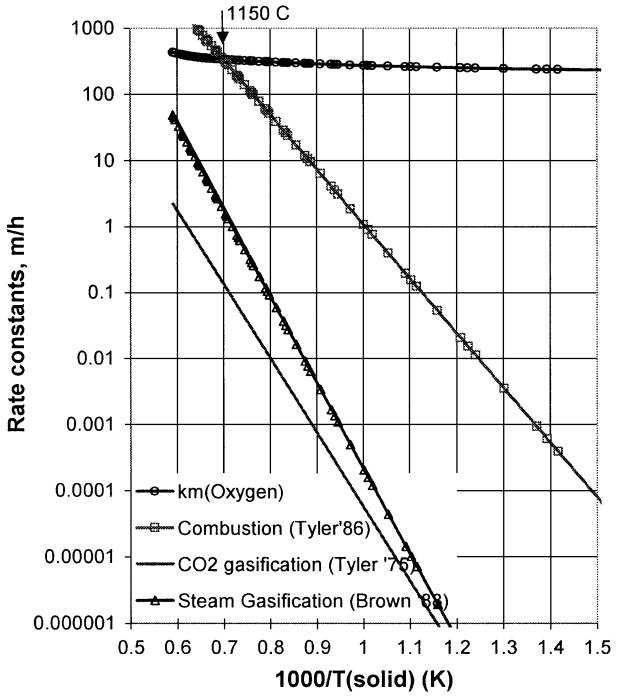

Fig. 2. Comparison of the petcoke combustion and gasification rate constants' dependence on temperature. The film mass-transfer rate coefficient, k_m, estimated using the correlation of Gupta and Thodos [23] is also known.

In addition to the above reactions, the combustion of CO and H_2 can occur in the combustion zone. Yoon et al. [5] reported that their extent is unclear given the short gas residence time in this zone. Denn and Shinnar [12] say that while the H_2 free-radical combustion reaction can be expected to occur rapidly in the combustion zone, ash and char surfaces can quench this reaction. The concluded that the presence/absence of these gas-phase combustion reactions have little effect on reactor effluent properties, as is borne out from several studies that are able to accurately predict syngas composition without including these reactions in their models. We too have assumed that these reactions can be neglected without introducing significant error.

5. Mass-transfer effects

Apparent rates in moving bed gasification models should include intrinsic reaction rate, pore diffusion rate, and bulk film diffusion rate. Yoon et al. [5] proposed two physical models for coal particle behavior in moving bed gasifiers. The first is called the Shell Progressive (SP) Model which assumes that ash retains its structure and remains on the reacting coal particle and thereby contributes to the film diffusion rate. The second is called the Ash Segregation (AS) Model where it was assumed that the ash falls off the coal particle and there is no ash layer between the coal particle and the gaseous reactants. True

ash behavior can be expected to lie in between these two limiting cases. Petcoke contain low ash levels compared to coals, and thus, the present model assumes no diffusion limitation due to ash. If we assume that the contribution of reactions within the pores is negligibly small, the following simple mathematical description of film diffusion followed by surface reaction can be written

$$\mathrm{Rate}_{\mathrm{net}} = \frac{A_{\mathrm{C}} \mathrm{C}_{\mathrm{bulk}}}{\left\{ \frac{1}{k_{\mathrm{g}}} + \frac{1}{k} \right\}} \tag{7}$$

where k is the intrinsic reaction rate, A_{c} is the specific coke surface area per unit reactor volume, k_{g} is the bulk gas-phase mass transfer coefficient (m/h), and C_{bulk} is the reacting gas concentration at the particle surface. The specific coke surface area at any specific location in the bed depends on the particle diameter, bed voidage, and overall conversion of coke. The assumption that the apparent rates are surface-controlled and that the contribution of reaction within the pores is small can be expected to hold at higher temperatures when the intrinsic reaction rates are high and pore diffusion limitation is significant. This assumption is thus expected to allow good prediction of petcoke gasification kinetics for operation under slagging conditions.

The bulk film mass-transfer coefficient has been estimated using the correlation of Gupta and Thodos [23]. This correlation has been used in several MBG modeling studies [6,7]. The bulk film heat-transfer coefficient was estimated from the correlation of Gupta and Thodos [23] for nonreacting packed beds.

6. Volatilization model

Petcoke volatile content is typically below 10 wt.%, and volatiles thus have a relatively smaller impact on product syngas composition in comparison to most coals. As mentioned above, we have adopted the volatilization reaction scheme proposed by Bliek et al. [10]. They presented a detailed model for single spherical particles undergoing volatilization and modeled the effect of intrinsic volatilization kinetics and pore diffusion resistance on net volatilization rates. They found that volatilization rates are strongly influenced by heating rates and particle diameter. Typical heating rates in moving bed reactors are 0.2–1 °C/s. At such heating rates, volatilization should be predominant in the temperature range 200–500 °C, and pore diffusion resistance is likely to be significant, especially for larger particles.

Bliek et al. [10] presented fraction volatilization versus temperature data at constant heating rates for heating rates varying from 0.5 °C/s to 500 °C/s, and for particles of diameter 0.01 to 3 cm. We found that the following equation allows fair agreement with their volatilization data.

$$\frac{\mathrm{d}v_i}{\mathrm{d}T} = \frac{v_{\mathrm{i}} h}{\left\{ \frac{1}{k_{\mathrm{vi}}} + \frac{\sqrt{\mathrm{d}_{\mathrm{p}}}}{k_{\mathrm{p}}} \right\}} \tag{8}$$

Table 3
Intrinsic volatilization kinetic parameters from Bliek et al. [10]

$k_{vi}=k_v^0 e^{-E/RT}$	k_v^0 (1/h)	E (kJ/mol)
Reaction (volatiles to gas)	93	2.88E08
Reaction (volatiles to tar)	188	2.73E15
Reaction (tar to gas and soot)	60	9.72E07

Here, v_i is the volatile carbon fraction (gas-forming, tar-forming, or tar), T is temperature, and h is the heating rate. k_{vi} are the intrinsic volatilization rates and k_p is a pore mass-transfer coefficient. We used the intrinsic volatilization kinetic parameters of Bliek et al. [10], as listed in Table 3, and an inverse square root dependence on particle diameter to account for pore mass-transfer resistance. Bliek et al.'s [10] data at low heating rates and for 1–3 cm diameter particles were used to obtain k_p values for our gasifier model. The volatilization rate expressions in the gasifier model are,

$$R_{v,i}(\mathrm{kmol/m^3/h}) = \frac{\rho_s \left\{ \dfrac{\mathrm{mvc_i}}{\mathrm{mvc_{ifeed}}} \right\}}{\left\{ \dfrac{1}{k_{vi}} + \dfrac{\sqrt{\mathrm{d_p}}}{k_p} \right\}} \tag{9}$$

where ρ_s is the molar coke density and mvc and $\mathrm{mvc_{feed}}$ are the molar volatile carbon flow rates.

Fig. 1 shows the stoichiometry of the volatilization reactions in our model. In the volatile carbon-to-gas reaction (r_{vg}) there are four unknown stoichiometric coefficients, α_1, β_1, γ_1, and δ_1, and three constraints for the mass balance of C, H, and O. Rhinehart et al. [26] give typical coal volatilization yields of methane, CO_2, CO, and H_2, the gases constituting the bulk of the gases produced. The range of volatilization yields in g/g coal for these components were: methane, 0.011–0.016; CO_2, 0.007–0.26; CO, 0.005–0.027; and H_2, 0.027–0.17. We have set CO formation to zero (γ_1=0) for petcoke gasification and determined α_1, β_1, and δ_1 from mass balance. The tar-to-gas reaction (r_{tg}) has a soot formation coefficient, q, as an additional parameter. For petcoke gasification we have set this to 0.8, γ_2=0, and again obtained α_2, β_2, and δ_2 by mass balance.

Volatile carbon, tar, and soot are assumed to combust/gasify with intrinsic rate constants identical to that of fixed carbon. The respective active specific surface area is estimated from the species and total feed carbon molar flows, the reactor voidage, and effective particle diameter. The bulk gas O_2, CO_2, or H_2O concentrations are used for combustion, CO_2, or steam gasification, respectively.

$$r(\mathrm{kmol/m^3/h}) = \frac{\left(\dfrac{6}{\mathrm{d_{p,eff}}} \right) \left\{ \dfrac{\mathrm{mvcg/mvct/mt/ms}}{\mathrm{mfc_{feed} + mvcg_{feed} + mvct_{feed}}} \right\} (1-\varepsilon_C) C_{O_2/CO_2/H_2O}}{\left\{ \dfrac{1}{k_i} + \dfrac{1}{k_m} \right\}} \tag{10}$$

7. Mathematical model and solution technique

Moving bed gasification reactors involve countercurrent flow of solids and gases, with feed solids and gases entering at opposite ends of the reactor. Our model assumes that solid and gas compositions and temperatures in the bed are radially uniform. Axial dispersion is assumed negligible in both phases, resulting in countercurrent plug flow. Cylindrical geometry is considered. Other assumptions made are particles undergo devolatilization, combustion and gasification simultaneously, ideal gas, single feed particle size, and uniform particle size at any bed height.

The differential equations describing this type of process represent a two-point boundary value problem. We have used the method of orthogonal collocation on finite elements to solve the model equations. The simulations presented here used a bed height of 7.2 m with a total of 80 equally spaced nodes, resulting in a grid spacing of 0.09 m. Simulations were also carried out with finer grid spacing of 0.025 m in the bottom 2 m of the bed where the combustion reactions lead to very high reaction rates. However, the uniform grid spacing of 0.09 m used allowed similar accuracy and numerical stability and is more efficient with respect to computation time. Detailed examination of existence of multiple steady states was not conducted. The simulations however showed the presence of a second low-temperature steady state where fixed carbon combustion reactions do not occur.

The individual species comprising the solid and gas phases and the gas and solid temperatures are declared as distributed variables in the model. Differential equations are written for each of these variables obtained from the respective material and energy balances. For steady-state simulations, the model equations can be represented as follows. Material balance for gas and solid material flow rates give,

$$0 = \frac{\mathrm{d}m_{\mathrm{i}}}{\mathrm{d}z} - A_{\mathrm{t}} \Sigma v_{\mathrm{ij}} R_{\mathrm{i}} \tag{11}$$

Energy balance for gas and solid temperatures gives,

$$0 = \sum_{i(\mathrm{gas})} m_{\mathrm{i}} c_{\mathrm{pi}} \frac{\mathrm{d}T_{\mathrm{g}}}{\mathrm{d}z} - A_{\mathrm{t}} \Sigma R_{\mathrm{i}} \Delta H_{\mathrm{i}} - A_{\mathrm{t}} A_{\mathrm{c}} k_{\mathrm{h}} \left(T_{\mathrm{g}} - T_{\mathrm{s}}\right) - k_{\mathrm{q}} \left(T_{\mathrm{g}} - T_{\mathrm{w}}\right) \tag{12}$$

$$0 = \left\{ \sum_{i(\mathrm{solid})} m_{\mathrm{i}} c_{\mathrm{pi}} + \frac{4\sigma A_{\mathrm{t}} T_{\mathrm{s}}^3}{(2/\varepsilon - 1)} \right\} \frac{\mathrm{d}T_{\mathrm{s}}}{\mathrm{d}z} - A_{\mathrm{t}} A_{\mathrm{c}} k_{\mathrm{h}} \left(T_{\mathrm{g}} - T_{\mathrm{s}}\right) \tag{13}$$

Heat released/absorbed in various reactions are assumed released in the gas phase. Heat exchange between gas and solid and between gas and coolant in the reactor jacket is included in the above equations. Energy balance for solids includes axial radiative heat transfer between adjacent solid layers.

Table 4
Model parameters

ρ_s	450 kg/m^3
k_h	15 kJ/m^2/h/K
k_q	1884 kJ/m/h/K
σ	20.4 10^{-8} kJ/m^2/h/K^4
ε	0.75
ε_C	0.35
k_p	10 h^{-1}
fr_vcg	0.4
fr_n2	0.6
q	0.8

Input parameters to the model include reactor dimensions, feed gas and coke flow rates, composition, pressure, and temperature, coolant temperature. Calculated quantities include axial profiles of gas and coke flow rates, composition, pressure, and temperature, axial variation of reaction rates, wall heat loss, gas and solid mean residence times, and syngas heating value (HV). Table 4 gives model parameter values used in our simulations.

8. Simulation of slagging gasifiers

In typical dry ash operation of moving bed gasifiers, high steam-to-carbon feed rates are used to keep maximum bed temperatures below 1200 °C. This mode of operation suffers from low coal/coke throughputs and low thermal efficiency due to high steam feed rates. Reduction of steam feed rate allows operation at higher temperatures, allowing increased kinetics and higher solid throughputs, better thermal efficiency with lower CO_2, and higher CO in syngas produced. Bed temperatures exceed 1200 °C leading to ash melting and slag formation. Petcoke are difficult to combust due to their low volatile and high fixed carbon content and require the high temperatures attained when operating with low steam feed rates for its combustion.

Simulation of coal gasification in moving bed reactors has been widely reported and discussed in the literature [5–9]. Reports on petcoke/coke gasification in moving bed reactors are however scanty in comparison. Lacey [27] and Hebden et al. [28] reported a slagging gasifier operation at Solihull, England, using various coals and coke as feedstock. Yoon et al. [5] developed a model for coal gasification and simulated the Solihull gasifier operation at slagging conditions. They reported that in slagging zone operation, coal throughputs about three times that in Lurgi dry ash gasifiers could be attained. Even higher throughputs of four to seven times were claimed in the pilot-plant operations by Lacey [27] and Hebden et al. [28]. They estimated peak temperatures approaching 2000 °C in a narrow 1 m band at the very bottom of the bed from their model. Gas and solid temperatures were assumed to be the same in their model. We have used the model developed here to examine in greater detail moving bed gasification of petcoke under low steam and oxygen slagging conditions and compared these results with entrained flow reactor data.

8.1. Model validation with coke gasification data

Operating data for the slagging gasifier at Solihull, England, have been reported by Lacey [27]. The slagging zone operation data for Avenue coke and Donisthorpe coal (a bituminous coal) were used by us for validation of the model described above. Table 5 gives the proximate and ultimate analyses of the two carbon feed stocks and the operating conditions for these slagging gasifier tests. The proximate data indicate that the avenue coke composition is quite similar to that of typical petcokes, being high in fixed carbon and low in volatile carbon. We simulated two tests (test #54 and test #67) using the same combustion and gasification kinetic parameters discussed earlier. Table 6 gives a comparison of the model simulation results with the plant operating data. The simulated values for the exit gas composition and exit ash temperature are seen to be in good agreement with plant data for Avenue coke. Simulated results for gasifier temperature and flow profiles are shown in Figs. 3–5. The gas temperature is seen to peak at a height of 27 cm from the bottom of the bed, and the fixed carbon combustion/gasification reactions are almost complete within the bottom 50 cm of the bed, where the solid temperature exceeds 1200 °C. These results are also in good agreement with the simulation results of Yoon et al. [5] for the same data. The model shows that volatile carbon conversion to tar and gas occurs in the top half of the bed where solid temperatures reach 700 °C. Tar converts to gas and soot in the middle of the bed, while soot is gasified in the hot zone in the bottom of the bed alongside fixed carbon.

Table 5
Solihull gasifier data Lacey [27]

	Test #54 Avenue coke	Tes #67 Donisthorpe
Coal properties		
Composition (moisture free basis, wt.%)		
Fixed carbon	82.34	54.50
Volatile carbon	10.11	38.15
Ash	07.55	07.35
Ultimate Analysis (moisture free basis, wt.%)		
C	88.00	71.30
H	00.75	05.00
N	01.05	01.55
S	01.15	01.45
Cl	00.05	00.15
O	01.45	13.20
Ash	07.55	07.35
Weight fraction moisture as charged	09.45	12.70
Operating conditions		
Operating pressure	21.4 atm	21.4 atm
Gas feed temperature	371 °C	371 °C
Coal feed rate (maf; kg/m^2/h)	2512	4788
Gas feed rate		
O_2 (kg/m^2/h)	1731.6	2278.8
H_2O (kg/m^2/h)	1141.2	1407.6

Table 6
Simulation of Solihull slagging gasifier [27]

	Avenue coke			Donisthorpe	
	Test #54	Model		Test #67	Model
Product gas composition (mol.%, dry)			Product gas composition (mol.%, dry)		
CO	70.45	68.79	CO	61.30	55.38
H_2	27.25	24.05	H_2	28.05	34.01
CO_2	01.85	02.82	CO_2	02.55	03.76
CH_4	00.45	02.47	CH_4	07.65	04.77
Exit slag temperature	1345 °C	1384 °C	Exit slag temperature	1330 °C	1420 °C
Max temperature	–	1869 °C	Max temperature	~2000 °C[a]	1830 °C
Height above grate at which max. temp. is reached	–	27 cm	Height above grate at which max. temp. is reached	9 cm[a]	27 cm

[a] As simulated by Yoon et al. [5].

The syngas flow profiles show rapid utilization of feed oxygen and steam in bottom 1 m of the bed, with a corresponding rise in CO_2, CO, and H_2. The CO_2 profile shows a sharp peak followed by a rapid decrease due to depletion of oxygen and CO_2 utilization in gasification reaction. The CO_2 production increases towards the top of the bed due to volatilization of volatile carbon and via the forward WGS reaction. Methane flow is seen to increase towards the top of the bed from volatilization of volatile carbon.

Simulation of Donisthorpe coal gasification gave lower exit gas CO and CH_4 and higher H_2 than plant data. The stoichiometry of volatization that yields to CH_4, CO, and CO_2 can vary significantly for different types of coals and can explain this deviation. The maximum gas temperature calculated by our model is 1830 °C, which is lower than the maximum gas+solid temperature of ~2000 °C calculated by Yoon et al. [5]. The high

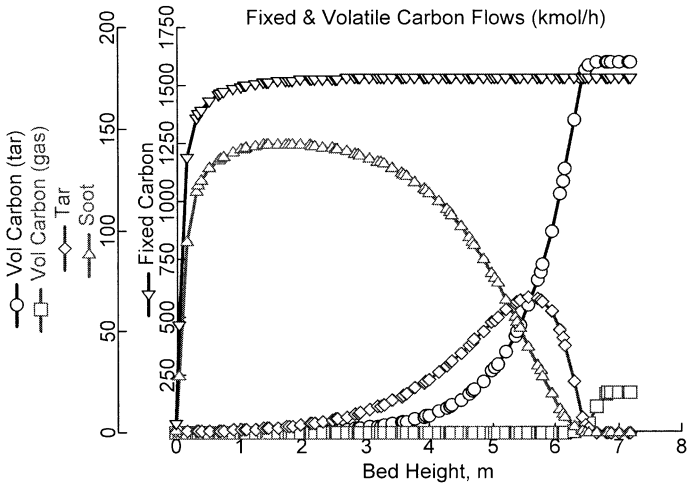

Fig. 3. Fixed and volatile carbon flow profiles for gasification of Avenue coke.

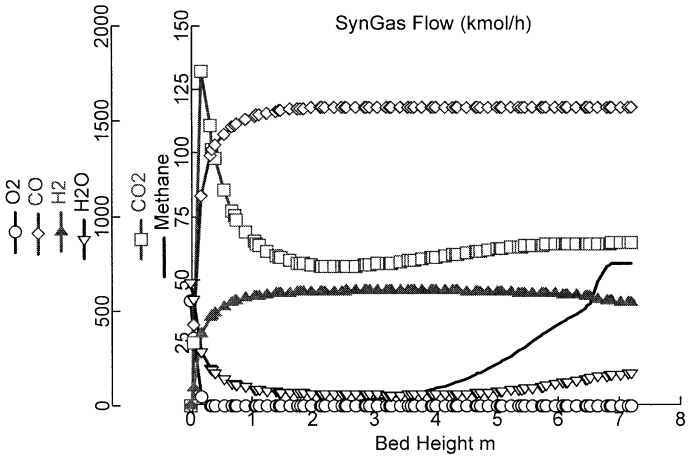

Fig. 4. Syngas flow profiles for gasification of Avenue coke.

volatile carbon levels in this coal resulted in a significant amount of it reaching the combustion zone and getting combusted/gasified at the bottom of the bed.

The model was also validated with gasification data for a high volatiles and high ash Indian coal. The data were generated in a 1.14-m diameter Lurgi dry ash gasifier operating with steam/C ratio in the range 0.7–1.5 and O_2/C in the range 0.2–0.3. These simulations used kinetic parameters for lignite coals. Simulation results for low-pressure air gasification, as well as high-pressure oxygen gasification, were seen to be in fairly good agreement with pilot plant exit syngas composition and temperature data. Thus, the present model was found to allow accurate simulation of gasifier operation over a wide range of operating conditions.

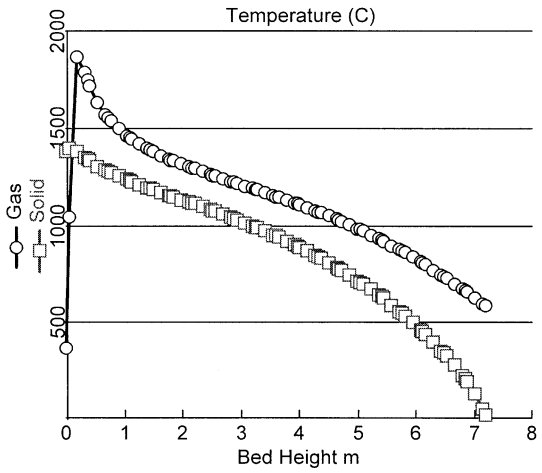

Fig. 5. Gas and solid temperature profiles for gasification of Avenue coke.

8.2. Petcoke gasification: effect of variation of feed O_2/C and steam/C ratios

Table 7 gives the operating conditions selected for simulation of slagging zone petcoke gasification. The petcoke composition used for these simulations was obtained from the petcoke proximate and ultimate analyses given in Table 1. The gasifier dimensions used were: diameter=3.6 m, height=7.2 m. Operating pressure: 28 bar. The oxygen and steam to maf petcoke molar ratios (represented as O_2/C and Steam/C, respectively) were varied in the range 0.26–0.32 and 0.26–0.34, respectively. The range covered roughly corresponds to substoichiometric levels of combustion and gasifying agent, resulting in incomplete conversion of petcoke. This was deliberately done to examine the effect on petcoke conversion.

The feed petcoke rate was selected to be 1000 TPD maf petcoke, with resulting petcoke flux of 4093 kg/m^2/h. This is three to four times higher than typical solid flux in dry-ash gasifiers, as shown in Table 8, which lists fluxes in several commercial moving bed gasifiers. The Ruhr and BG gasifiers are slagging gasifiers and report solid flux of 3800 and 4750–5550 kg/m^2/h, respectively. The Lurgi (Dravo) gasifier reports an unusually high flux of 3200 kg/m^2/h for a dry-ash gasifier.

The simulation results for petcoke conversion, syngas composition, flow and energy density, mean gas and solid residence time, exit gas and solid temperature, and maximum gas temperature for feed O_2/C=0.32 and Steam/C=0.3 are also shown in Table 7. Petcoke conversion of 97.23% is simulated. Mean gas residence time is 29.5 s, and mean solid

Table 7
Base case MBG petcoke gasification simulation

Operating conditions		Simulation results		
d_p	0.02 m		Units	Value
D_{bed}	3.60 m	Coke conversion		97.23
H_{bed}	7.20 m	Gas mean residence time	s	29.52
t_s (feed)	25 °C	Solid mean residence time	h	0.635
t_g (feed)	300 °C	Wall heat loss	GJ/h	18.14
Pressure	28 bar (reactor bottom)	HV syngas	GJ/h	1219.14
			MJ/Nm^3	12.06
Petcoke (proximate and ultimate analyses from Table 1)		Syngas flow	Nm^3/h	101096
Feed rate	46,175 kg/h		H_2O free syngas composition	
	(≡1000 TPD maf petcoke)		CO	0.5939
Feed gas			CO_2	0.0399
O_2/C	0.32 mole/mole maf petcoke		H_2	0.2992
Steam/C	0.30 mole/mole maf petcoke		CH_4	0.0376
			H_2S	0.0147
O_2 concentration: 96% (balance N_2)			NH_3	0.0035
		T_g (exit)	°C	911.01
		T_g(max)	°C	1957.58
		T_s (exit)	°C	1438.2
		CO/H_2 ratio		1.99
		Pressure drop	bar	0.16

Table 8
Commercial moving bed gasifier capacity and flux rates [30]

	BGL slagging	Ruhr	Lurgi–Dravo	IICT[a]	METC	GE gas
Capacity, TPD	300–350	168	800	137.5	24	24
Diameter, m	1.83	1.5	3.65	1.13	1.06	1.37
Flux, kg/m^2/h	4750–5550	3800	3200	900	1100	676

[a] Krishnudu et al. [31].

residence time is 0.63 h. H_2O free syngas has 59.39% CO, 29.92% H_2, 3.99% CO_2, 3.76% CH_4, and 1.47% H_2S, and it has a heating value (HV)[1] of 12.06 MJ/Nm^3.

The simulation results showing effect of feed O_2/C and Steam/C variation are shown in Figs. 6–8. Petcoke conversion is seen to increase with increase in O_2/C and Steam/C feed ratios. Conversion dependence on the steam/C ratio is, however, indicated to be considerably weaker than on the O_2/C ratio and appears to be insignificant at O_2/C ratios below 0.26.

Bed exit gas temperatures are not significantly changed by the changes in O_2/C ratio and Steam/C ratios. The maximum gas temperatures and the exit solid temperatures both decrease with increasing steam/C ratio. The exit solid temperatures increase with increasing O_2/C ratio. These trends can be explained on the basis of the exothermicity of the combustion reaction versus the endothermicity of the steam-gasification reaction. The maximum solid and gas temperatures occur at a distance of 0.09–0.18 and 0.27–0.45 m, respectively, from the bed bottom. The variation in O_2/C and Steam/C had no effect on the location of the maximum temperatures for the range studied. The solid temperature does not decrease significantly from the peak value.

The H_2O free syngas has about 85–90% CO and H_2. The CO/H_2 ratio increases with O_2/C. The CO/H_2 ratio lies in the range 1.5–2.1 for the conditions studied. The H_2O free syngas heating value (HV) increases with an increase in O_2/C and decreases with an increase in Steam/C, and it lies in a fairly narrow band of 11.4–12.2 MJ/Nm^3 for the conditions examined. For complete petcoke conversion with stoichiometric oxygen and steam, syngas HV increases with increasing O_2/C ratio in the range 0.26–0.34. At even higher O_2/C ratios, this trend is likely to reverse due to a decrease in the partial combustion products CO and H_2.

These results can be useful in selecting feed gas oxygen and steam flows with respect to operational issues such as optimization of gasifier thermal performance, syngas CO/H_2 ratio required from downstream processing requirements, maximum gasifier temperatures allowable for a specific refractory, etc. The steam to oxygen feed ratio serves as the primary control variable for gasifier temperature control. Blast/feed gas temperature is also used for temperature control.

8.3. Petcoke gasification: gasifier capacity

The effect of higher petcoke throughputs was examined for operation at base case conditions. Fig. 9 shows a variation in petcoke conversion, gasifier pressure drop, gasifier

[1] Heating value calculated using heats of combustion of CO, H_2, and CH_4.

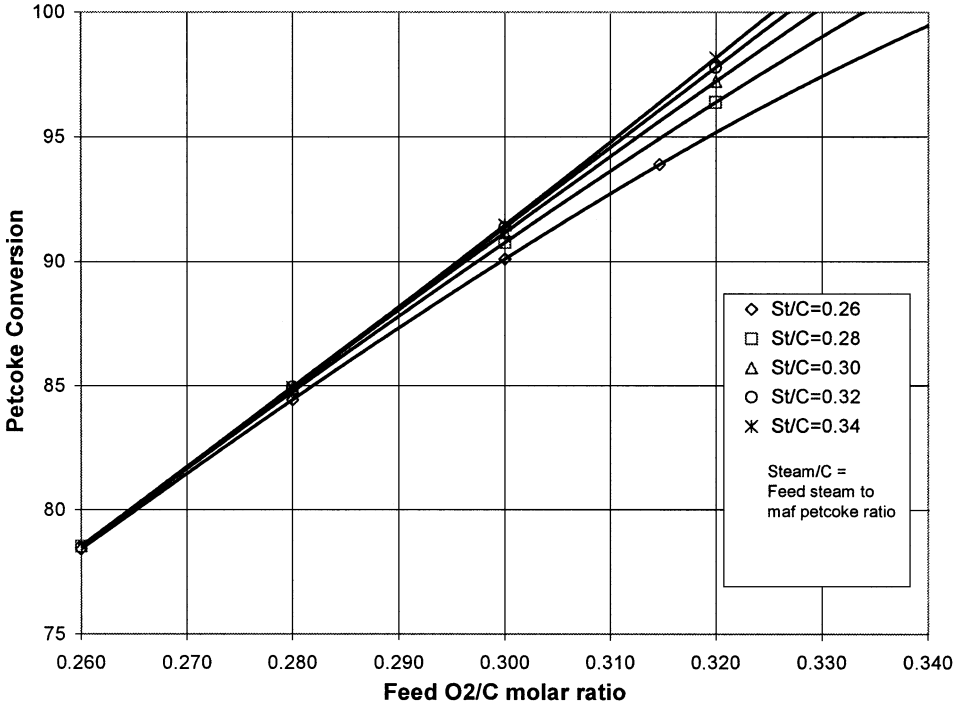

Fig. 6. Effect of feed O_2/C and Steam/C flow ratios on petcoke conversion at the base case operating conditions.

exit gas and solid temperatures, and max gas temperature with increase in feed petcoke flow from 1000 to 2000 TPD maf petcoke (flux increase from 4093 to 8186 kg/m^2/h). Petcoke conversion drops from 97.23% to 87.03%, gas residence time drops from 29.5 to 12.2 s, solid residence time drops from 0.63 to 0.32 h, and pressure drop increases from 0.16 to 0.66 bar[2] (0.022–0.092 bar/m). Gas phase temperatures increase with increased throughput: maximum gas temperature increases from 1957 to 2199 °C, while exit gas temperature increases from 911 to 1323 °C. Exit solid temperatures decrease marginally from 1438 to 1409 °C.

The relatively small drop in conversion with doubling in petcoke flux indicates that the slagging MBG process is not kinetically limited at these flux rates. However, gas–solid flow hydraulic limitations are likely to arise at these high flux rates. The mean gas superficial velocity for the base case is 0.24 m/s while that for 2000 TPD petcoke flow is 0.59 m/s. Minimum bed fluidization velocities estimated using the correlation of Kunii-Levenspeil [29] at 1500 °C temperature, and 28 bar pressure for petcoke particles of 2 and 0.25 cm (which would roughly correspond to 99.2% conversion of a 2-cm feed petcoke particle) are 1.48 and 0.42 m/s, respectively. This suggests that at a petcoke flux of 8200 kg/m^2/h, fluidization of the smaller particles would occur resulting in their being blown out of the combustion zone. Operation at higher gasifier

[2] Hobbs et al. [7] reported dry-ash MBG pressure drops in the range 0.0025–0.015 bar/m, albeit at a significantly lower solid flux of 260–875 kg/m^2/h.

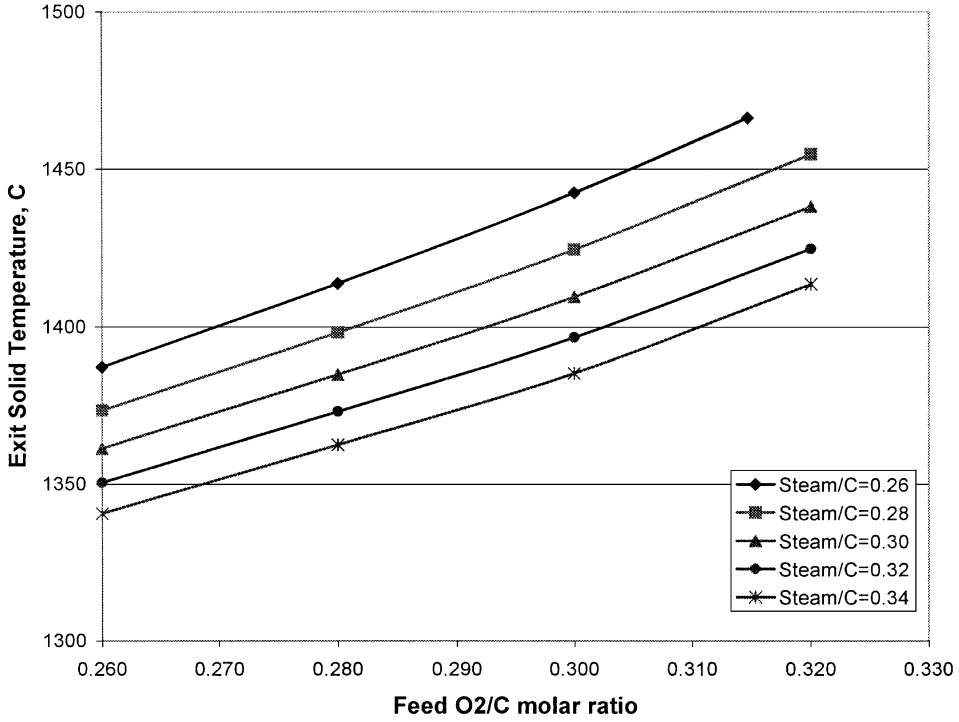

Fig. 7. Effect of feed O_2/C and Steam/C flow ratios on exit solid temperature at the base case operating conditions.

pressures allows reduction in gas superficial velocity. However, this also results in lower minimum fluidization velocities. The above analysis suggests that hydraulic limitations are likely to prevent operation at fluxes significantly higher than 5000 kg/m^2/h. The highest solid flux reported in commercial operation is for the BGL slagger at 5550 kg/m^2/h [30].

8.4. Petcoke gasification: effect of variation in model parameters

The relative magnitudes of the combustion and gasification rates can have considerable impact on gasifier temperatures and coke conversion. The combustion rate was seen to be mass-transfer limited at temperatures above 1150 °C in Fig. 2. Thus, variation in the combustion kinetic parameters should not have significant impact on slagging gasifier performance. Use of petcoke kinetic parameters given by Walsh and Green [17] with activation energies of 112 and 171 kJ/mol (see Table 2) gave similar results to those obtained with the Tyler [15] parameters for base case conditions. However, the steam and CO_2 gasification rates are not mass-transfer limited. Higher gasification rates lead to lower gas and solid temperatures. Coke conversion is higher despite the lower solid temperatures. For the base case condition, doubling both the steam and CO_2 gasification rate constants ($k_{o,2}$, $k_{o,3}$) simultaneously by 100% leads to a conversion increasing to 98.4%

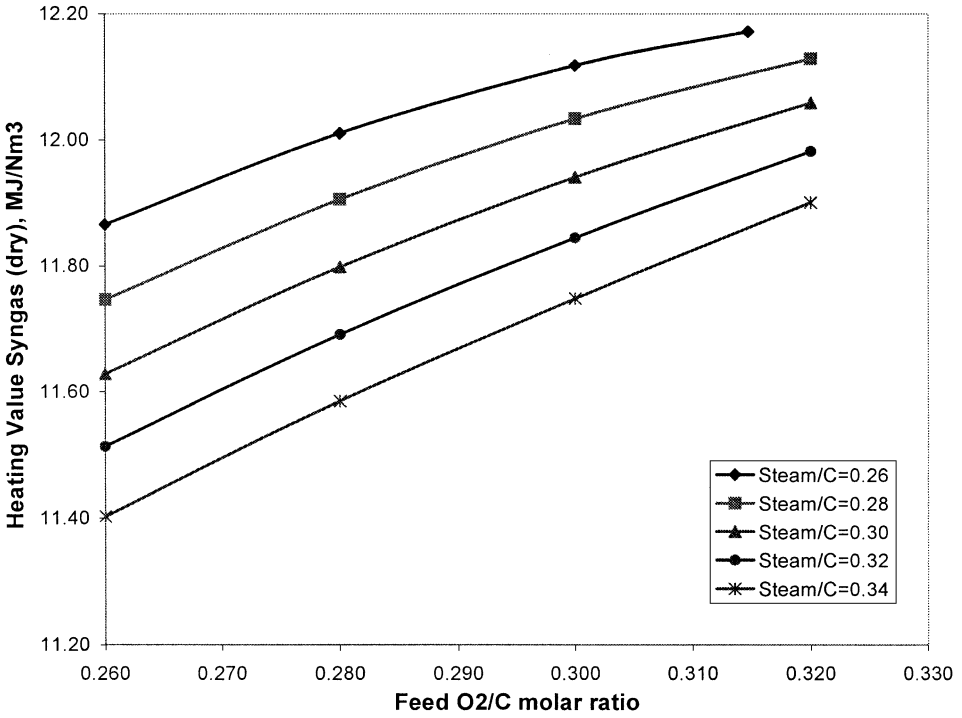

Fig. 8. Effect of feed O_2/C and Steam/C flow ratios on syngas heating value at the base case operating conditions.

and to a decrease of exit gas, peak gas, and solid temperatures by 25, 85, and 45 °C, respectively. The syngas compositions are practically unchanged by these variations in rate constants.

The variation of coke conversion with the feed steam/C ratio was seen to be quite weak in Fig. 6. Higher CO_2 gasification rate constants give a higher sensitivity of coke conversion to the feed steam/C ratio. Higher feed steam levels increase the forward WGS reaction rate and CO_2 production, which then participates in the CO_2 gasification reaction.

The reported WGS rate constants at temperatures in excess of 1200 °C are high enough to ensure equilibrium. However, at temperatures below 1000 °C, the exit syngas composition is sensitive to variations in the WGS reaction rate. Reported low temperature WGS rates (Table 2) show considerable variation. The rates obtained from Biba et al.'s [8] rate parameters would give an equilibrium even at the lower temperatures, resulting in high CO_2 prediction. However, lower rates estimated from the other three citations result in the WGS reaction not being in equilibrium. Use of rates significantly lower than those of Bhattacharya et al. [24] at the lower temperatures does not have a significant impact on the exit gas composition.

Hobbs et al. [7] report that the gas–solid heat transfer coefficient for reacting systems can be 10–50 times lower than for nonreacting systems. Their data from dry-ash gasifiers gave heat-transfer coefficient magnitudes 2–10% of those from Gupta and

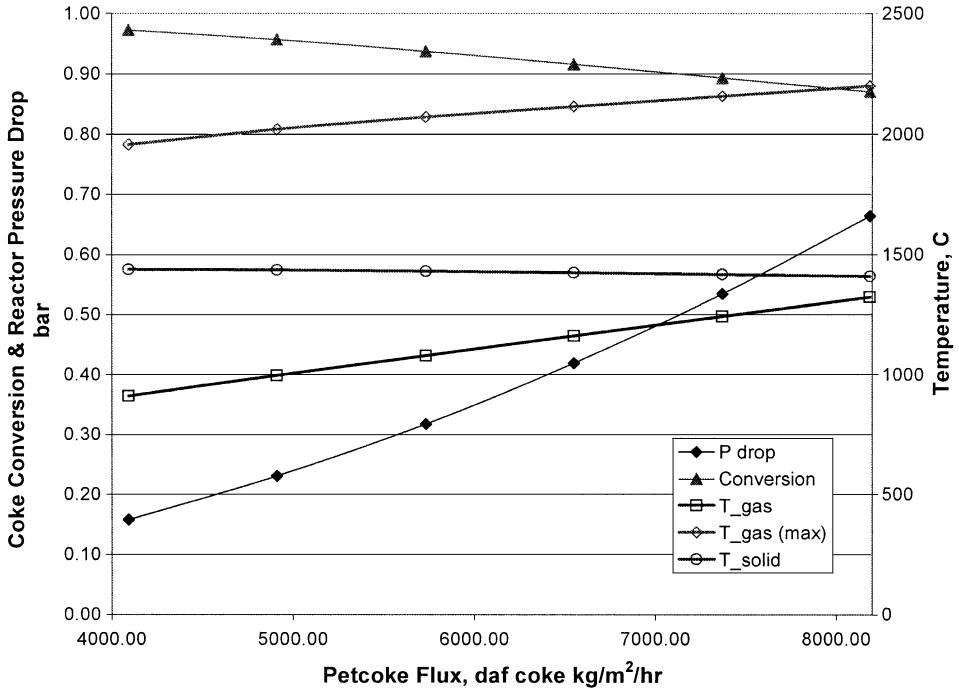

Fig. 9. Effect of feed petcoke flux on coke conversion, reactor pressure drop, reactor exit gas, maximum gas, and exit solid temperatures at the base case operating conditions of Table 7.

Thodos [23], derived for nonreacting packed beds. In slagging gasifiers with their high reaction rates, the heat-transfer coefficient magnitude can be expected to be still lower. A constant value of the gas–solid heat transfer coefficient (k_h=15 kJ/m^2/h/K) was used in the simulations. This was about 1% of the value obtained from the heat-transfer correlation of Gupta and Thodos [23]. For the base case conditions, doubling the value of k_h resulted in the mean gas–solid temperature difference in the bed dropping from 488 to 276 °C. The solid temperatures increased with the exit solid temperature rising to 1486 °C, leading to a higher conversion of 99.6%. Peak gas and exit gas temperatures were lower at 1770 and 771 °C, respectively. Syngas composition was not significantly altered. Thus, gasifier temperature profiles are quite sensitive to the gas–solid heat transfer coefficient.

8.5. Petcoke gasification: comparison with EFG performance data

Several commercial entrained flow gasifier (EFG)-based plants are presently operating around the world. Vis-à-vis EFGs, slagging MBGs are known to operate closer to thermodynamic optimum and allow operation at equivalent or better thermal efficiency with lower oxygen consumption. Oxygen plants represent a significant cost element in gasification plants, and reduction in oxygen requirement can bring down investment and operating costs.

Table 9
Comparison of moving bed gasifier performance with entrained flow gasifier

	EFG [4]	MBG: simulation results
Av. feed particle size, mm	0.1	20
Feed O_2/C, mol/mol (g/g)	−(1.038)	0.32 (0.764)
Feed steam/C, mol/mol (g/g)	−(0.24)	0.28 (0.376)
Coke conversion	99.5	99.4
HHV syngas, MJ/kg coke	25.61	28.9
Cold gas efficiency, %HHV	78.9	98[a]
Syngas flow, Nm^3/kg coke	1.79	2.38
T_g (reactor), °C	~1600	915.8 (exit gas)
H_2O free syngas composition:		
CO	0.6523	0.6027
CO_2	0.022	0.0361
H_2	0.259	0.2931
N_2+Ar+CH_4	0.0507	0.0383 (CH_4)
H_2S+COS	0.0158	0.0148 (H_2S)
NH_3	–	0.0035

Petcoke proximate and ultimate analyses as given in Table 1 for both EFG and MBG.
[a] Calculated from heat of combustion of CO, H_2, and CH_4 for syngas and C in feed petcoke.

EFGs use finely ground petcoke injected either as dry solids or as slurry. EFG performance data given in Kirk-Othmer [4] are compared with a simulated MBG performance using our model in Table 9. Similar carbon conversion levels are estimated possible with lower feed oxygen and higher feed steam. The use of higher steam along with a lower exit gas temperature results in a higher H_2/CO ratio in the product syngas for the MBG. The thermal performance of the MBG with over 20% less oxygen consumption is seen to be better than that of the EFG.

Entrained flow systems do not have separate combustion/gasification/volatilization zones, as is the case in MBGs. Petcokes typically contain about 10 wt.% volatiles, which are combusted in EFGs, leading to higher oxygen requirement. Excess oxygen is also used for combustion-based heating of the feed solids/slurry from ambient to reaction temperature. Volatile combustion produces steam, which allows reduction in external steam requirement for gasification reactions. The exit gas temperatures are higher for the EFG, allowing additional steam generation from syngas cooling.

In MBGs, the volatiles are gasified by thermal cracking in the absence of oxygen in the upper half of the bed. The feed solids are heated as they descend down the bed resulting in direct heat recovery from the syngas. This results in the lower exit syngas temperatures in MBGs. Internal heat recovery and direct gasification of volatiles result in significant advantages for MBGs over EFGs. EFGs, however, have the advantage of feed versatility being able to process liquid fuels in addition to finely ground solids.

9. Conclusions

A model for moving bed gasification of petcokes under slagging conditions was developed and validated using earlier reported data for coke/bituminous coal gasification

in a slagging gasifier. The model allowed accurate simulation of gasification of feedstock with widely varying levels of fixed/volatile carbon and ash, under slagging as well as dry ash conditions. The study suggests that under slagging conditions, these reactors can operate at very high petcoke flux in excess of 4000 kg/m^2, allowing MBG gasifiers to be sized comparable to entrained flow gasifiers (EFGs). Flux increase above 5000 kg/m^2/h is likely to be limited by high gas superficial velocities leading to fluidization of small particles near the bottom of the gasifier. The results indicate syngas composition and energy density similar to EFGs can be obtained in MBGs while operating with about 20% less feed oxygen, leading to potential savings from reduced oxygen plant size. Overall thermal efficiency (cold efficiency) of MBGs can be higher than of EFGs.

The simulations show that gas temperatures can approach 2000 °C in a narrow band near the bottom of the bed, an observation in agreement with an earlier slagging gasifier simulation study [5]. Such high temperatures can pose serious problems vis-à-vis refractory selection and life. Peak gas and solid temperatures can be lowered by increasing the feed steam/C ratio, although this leads to a reduced syngas heating value and a higher H_2/CO ratio. Controlling the peak temperature location above the grate is important to prevent formation of ash clinkers by resolidification in slagging gasifiers. Petcoke have low ash content, thereby reducing this controllability problem.

The model indicates that optimal oxygen utilization for gasification requires careful selection of reactor height for feedstock with high volatile carbon. Inadequate reactor height can result in volatiles breaking through to the combustion zone, thereby leading to excessive oxygen requirement or incomplete conversion of slower-reacting fixed carbon.

The present study concludes that slagging moving bed gasifiers hold promise for efficient gasification of petroleum cokes and that significant application potential exists for this route to petcoke-based syngas generation.

Nomenclature

A_t Bed cross-sectional area
E_a Activation energy
fr_n2 Fraction of N in fixed carbon that forms N_2
fr_vcg Fraction of volatile carbon that is gas-forming
fr_vct Fraction of volatile carbon that is tar-forming
k_o Arrhenius preexponential factor
k_q Coefficient of heat transmission from reactor
m Molar flow rates
R Gas constant
R_i Reaction rates
T_g Gas temperature
T_s Solid temperature
T_w Cooling water temperature
ΔH Heat of reaction
ε Emissivity of coke
v Stoichiometric coefficient
σ Stefan–Boltzmann constant

References

[1] Gasification Technologies Council, Gasification—worldwide acceptance and use, www.gasification.org, (2000 Jan.).
[2] P. Amick, R. Geosits, R. Herbanek, S. Kramer, J. Rockney, S. Tam. An optimized petroleum coke IGCC co-production plant. Presented at the Gasification Technologies Council Conference, San Francisco, CA, October 7–10, 2001.
[3] F.C. Jhanke, J.S. Falsetti, R.F. Wilson. Coke gasification: costs, economics, and commercial applications. Presented at NPRA Annual Meeting, San Antonio, Texas, March 17–19, 1996.
[4] J.I. Kroschwitz, M. Howe-Grant (Eds.), Kirk-Othmer-Encyclopedia of Chemical Technology, 4th ed. Gasification, vol. 6, John Wiley and Sons, 1993, p. 541.
[5] H. Yoon, J. Wei, M.M. Denn, A model for moving-bed coal gasification, AIChE J. 24 (5) (1978) 885.
[6] J. Adanez, F.G. Labiano, Modeling of moving bed coal gasifiers, Ind. Eng. Chem. Res. 29 (1990) 2079.
[7] M.L. Hobbs, P.T. Radulovic, L.D. Smoot, Modeling fixed-bed coal gasifiers, AIChE J. 38 (5) (1992) 681.
[8] V. Biba, J. Macak, E. Klose, J. Malecha, Mathematical model for the gasification of coal under pressure, Ind. Eng. Chem. Process Des. Dev. 17 (1) (1978) 92.
[9] D. Neogi, C.C. Chang, W.P. Walwender, L.T. Fan, Study of coal gasification in and experimental fluidized bed reactor, AIChE J. 32 (1) (1986) 17.
[10] A. Bliek, W.M. van Poel, W.P.M. van Swaaij, F.P.R. van Becker, Effect of intraparticle heat and mass transfer during devolatilization of a single coal particle, AIChE J. 31 (10) (1985 Oct.) 1666.
[11] N.M. Laurendeau, Hetrogeneous kinetics of coal char gasification and combustion, Pror. Energy Combust. Sci. 4 (1978) 221.
[12] M.M. Denn, R. Shinnar. Chemical reactor and reaction engineering. Chap. 8: Coal Gasification Reactors, p. 499, Marcel-Dekker, 1987.
[13] G.D. Sargent, I.W. Smith, Combustion rate of bituminous coal chars in the temperature range of 800 to 1700 °C, Fuel 52 (1975) 52.
[14] M.A. Gibson, C.A. Euker Jr. Mathematical modeling of fluidized bed coal gasification. Paper presented at AICHE meeting, Los Angeles, Calif. (1975 Nov.).
[15] R.J. Tyler, Intrinsic reactivity of petroleum coke to oxygen, Fuel 65 (1986 February) 235.
[16] I.W. Smith, Intrinsic reactivity carbons to oxygen, Fuel 57 (1978 July) 409.
[17] D.E. Walsh, G.J. Green, A laboratory study of petroleum coke combustion kinetics and catalytic effects, Ind. Eng. Chem. Res. 27 (1988) 1115.
[18] R.J. Tyler, I.W. Smith, Reactivity of petroleum coke to carbon dioxide between 1030 and 1180 K, Fuel 54 (1975 April) 99.
[19] B.W. Brown, L.D. Smoot, P.J. Smith, P.O. Hedman, Measurement and prediction of entrained flow gasification processes, AIChE J. 34 (3) (1988 Mar.) 435.
[20] S. Dutta, C.Y. Wen, R.J. Belt, Reactivity of coal and char: 1. In Carbon dioxide atmosphere, Ind. Eng. Chem. Process Des. Dev. 16 (1977) 20.
[21] D.A. Kairaitis, R.J. Tyler, Proc. Int. Conf. Coal Sci, Pittsburgh, 1983, p. 441.
[22] V.V. Revankar, A.N. Gokarn, L.K. Doraiswamy, Studies in catalytic steam gasification of petroleum coke with special reference to the effect of particle size, Ind. Eng. Chem. Res. 26 (1987) 1018.
[23] A.S. Gupta, G. Thodos, Direct analogy between mass and heat transfer to bed of spheres, AIChE J. 9 (6) (1963) 751.
[24] A. Bhattacharya, L. Salam, M.P. Dudukovic, B. Joseph, Experimental and modeling studies in fixed bed char gasification, Ind. Eng. Chem. Process des. Dev. 25 (1986) 988.
[25] H.Y. Sohn, R.L. Braun, Effect of internally generated bulk flow on rates of gas–solid reactions, Ind. Eng. Chem. Process des. Dev. 23 (1984) 691.
[26] R.R. Rhinehart, R.M. Felder, J.K. Ferrel, Dynamic modeling of a pilot-scale fluidized-bed coal gasification reactor, Ind. Eng. Chem. Res. 26 (1997) 738.
[27] J.A. Lacey, Gasification of coal in a slagging pressure gasifier, Adv. Chem. 69 (1967) 31.
[28] D. Hebden, J.A. Lacey, A.G. Horsler, Further experiments with a slagging pressure gasifier, Gas Council Research Communication GC112 (1964 Nov.).

[29] R.H. Perry, D.W. Green, J.O. Maloney, Perry's Chemical Engineers' Handbook, Sixth ed., 1984, p. 47, Chap.-9.
[30] R.D. Parekh, Handbook of Gasifiers and Gas Treatment Systems, Prepared by UOP/SDC for U.S. Dept. of Commerce, National Technical Information Service, (1982 Sept.).
[31] T. Krishnudu, B. Madhusudan, S.N. Reddy, V.S.R. Sastry, K.S. Rao, R. Vaidyeswaran, Studies in a moving bed pressure gasifier: prediction of reaction zones and temperature profile, Ind. Eng. Chem. Res. 28 (1989) 438.
[32] R.A. Olliver, J.M. Wainwright, R.F. Drnevich, Application of BGL Gasification of Solid Hydrocarbons for IGCC Power Generation, Presented at the Gasification Technologies Council Conference, San Francisco, CA, October 8–11, 2000.
[33] F. Bustamante, R. Enick, K. Rothenburger, B. Howard, A. Cugini, M. Ciocco, B. Morreale, Kinetic study of the reverse water gas shift reaction in high-temperature, high-pressure homogeneous systems, Fuel Chem. 47 (2) (2002) 663.